High Altitude Rocket Plume and Thermal Radiation Analysis

[Woo Jin Jeon, Seung Wook Baek, Jae Hyun Park and Dong Sung Ha]

***Abstract*—In this study, rocket plume behavior at various altitudes and radiative heat transfer to the base surface is investigated by using DSMC and Finite-volume method for radiation. Rapidly expanded plume with increasing altitude cause the low density transient flow region in the plume. And, because of the decrease of plume temperature and density, the radiative heat transfer to the rocket base surface is also decrease.**

***Keywords*—Rocket Plume, Base Heating, Direct Simulation Monte Carlo(DSMC), Finite Volume Method for radiation (FVM)**

I. Introduction

The density of atmosphere decreases as altitude increases, and it makes rocket experience continuum-transient-rarefied flow regime. The flow regimes are classified by Knudsen number (Kn) which means the ratio of molecular mean free path (λ) to characteristic length (L)[1]. If Kn is greater than 0.001 the flow is transient and the Navier-Stokes equation is not appropriate to solve this flow because it assumes that flow is continuum. In this study, the under-expanded rocket exhausted plume at altitude 30~80 km, whose atmospheric density is only 0.15% to 0.0016% of density at sea level.

II. Analysis Method

A. *DSMC Method*[1]

When the continuum assumption is not valid, the flow can be described by Boltzmann transport equation., Eq. (1).

$$\frac{\partial}{\partial t}(nf)+\vec{c}\cdot\frac{\partial}{\partial r}(nf)+\vec{F}\cdot\frac{\partial}{\partial c}(nf) = \int_{-\infty}^{\infty}\int_{0}^{4\pi} n^2\left(f^*f_1^*-ff_1\right)c_r\sigma\, d\Omega\, d\vec{c_1}. \tag{1}$$

However, Boltzmann equation is known too difficult to solve due to the collision term in right hand side, except the case that collision is neglected. Direct Simulation Monte Carlo(DSMC) method which directly describes molecules, is generally used instead of solving BTE analytically, and it was proved mathematically that the solution of DSMC is identical to the solution of BTE[2,3]. In DSMC, a simulated particle represents a number of real molecules. First, simulated particles are generated according to initial condition, then, these particles are moved and the new position of particles are calculated. The interaction between the particles and boundaries are applied during this phase. Next, the collisions between particles, energy exchange and redistribution of internal energy are calculated by applying collision model, and VHS(Variable hard Sphere) model[4] is applied here. After these movement and collision phase are repeated enough, the macroscopic properties of flow field are obtained by sampling of the microscopic properties of each particles in a cell. Bird's No Time Counter(NTC) method[1,5] is employed to sample. The Larsen-Borgnakke model[6], which assumes that part of collisions is inelastic and the rest is elastic, is used to model energy exchange.

B. *Finite Volume Method for Radiation*

Radiative heat flux is obtained by solving radiative transfer equation(RTE), Eq. (2), and axisymmetric RTE is employed[7-9].

$$\frac{1}{r}\frac{\partial(\mu r I)}{\partial r}-\frac{1}{r}\frac{\partial(\eta I)}{\partial \phi}+\frac{\partial(\xi I)}{\partial z} = \kappa_a I_b-(\kappa_a+\sigma_s)I+\frac{\sigma_s}{4\pi}\int_{\Omega'=4\pi} I\, d\Omega'. \tag{2}$$

where μ, η and ξ are the direction cosines of a path, and I_b, κ_a and σ_s are the black body intensity, absorption coefficient and scattering coefficient respectively. To obtain discretization equation, the RTE integrated over the control volume ΔV and

---

Woo Jin Jeon
Korea Advanced Institute of Science and Technology
Republic of Korea

Seung Wook Baek
Korea Advanced Institute of Science and Technology
Republic of Korea

Jae Hyun Park
Gyeongsang National University
Republic of Korea

Dong Sung Ha
Agency of Defense Development
Republic of Korea

control angle $\Delta\Omega^{mn}$. And then the discretization equation, Eq. (3) is obtained.

$$\sum_{i=1}^{N} I_i^{mn}\Delta A_i D_i^{mn} + (\Delta A_e D_e^{mn+1/2} + \Delta A_w D_w^{mn-1/2}) + (\kappa_a+\sigma_s) I_P^{mn}\Delta V\Delta\Omega^{mn} = S_P^{mn}\Delta V\Delta\Omega^{mn} \tag{3}$$

where ΔA is cell surface area, D_i^{mn} is the directional weigh and S_P^{mn} is source term. Rearranging Eq. (3) for I_P^{mn} the final Eq. (4a) is obtained.

$$a_P^{mn} I_P^{mn} = \sum_I a_I^{mn} I_I^{mn} + b_P^{mn} \tag{4a}$$

$$a_P^{mn} = \sum \max(\Delta A_i D_i^{mn},0) + (\kappa_a+\sigma_s)\Delta V\Delta\Omega^{mn} + \Delta A_e D_e^{mn+1/2} \tag{4b}$$

$$a_I^{m} = \max(-\Delta A_i D_i^{mn},0) \tag{4c}$$

$$b_P^{mn} = S_P^{mn}\Delta V\Delta\Omega^{mn} - \Delta A_w D_w^{mn-1/2} I_P^{mn-1} \tag{4d}$$

The subscript I represents the neighboring nodal point and i means the corresponding face. More detailed information about the axisymmetric FVM can be found in reference [9].

III. Result and Discussion

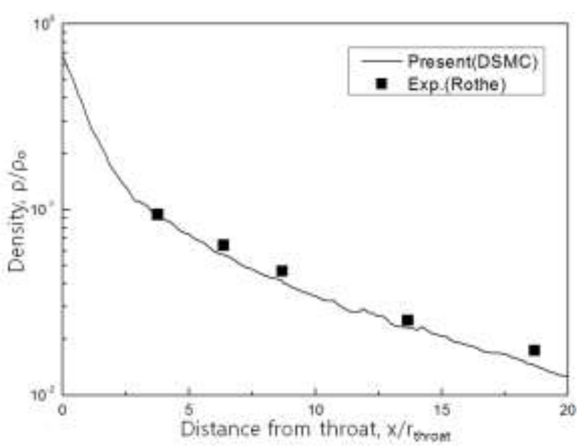

Figure. 1 Density variation along axis.

TABLE I. Test Condition

Species	N_2
Stagnation temperature	300 K
Stagnation pressure	474 Pa
Ambient pressure	1.5 Pa
Wall temperature	300 K

A. DSMC Code Verification

In this study, unstructured 2-dimensional axisymmetric DSMC code is employed. This code is verified using the empirical result of Rothe's nozzle[10]. The test conditions are in Table. 1. The Kn of atmosphere that the characteristic length is nozzle throat, is 0.023. The empirical result data and the numerical solution are compared in Fig. 1 and Fig. 2. The calculated solution shows similar result to the data. The rotational temperature shows higher value than translational temperature along the axis due to the rapid expansion.

B. FVM Code Verification

The verification for the 2-dimensional unstructured FVM code is carried out using exact and Monte Carlo solution of radiative heat transfer to the side walls of cylindrical and truncated conical enclosures with absorbing-emitting medium. In both cases, the medium temperature is 100 K and the wall is black and the temperature is 0 K. The medium has three different absorption coefficients(κ_a) for both cases. For the case of cylindrical enclosure, κ_a = 0.1, 1.0 and 5.0 m^{-1}, and for the case of truncated conical enclosure, κ_a = 0.1035, 0.270 and 1.035 m^{-1}. As shown in Fig.3 and Fig. 4, present FVM solutions are in good agreement with the exact and Monte Carlo solutions.

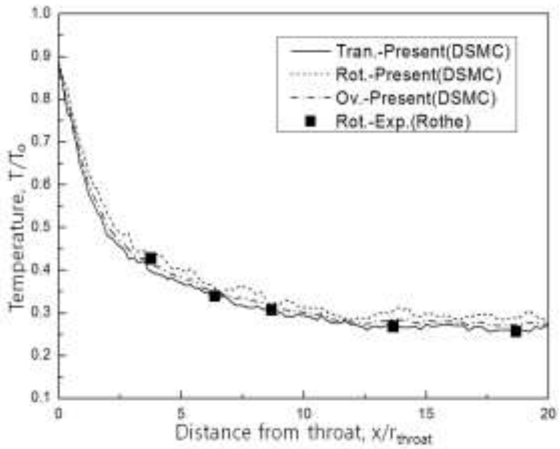

Figure. 2 Temperature variation along the axis.

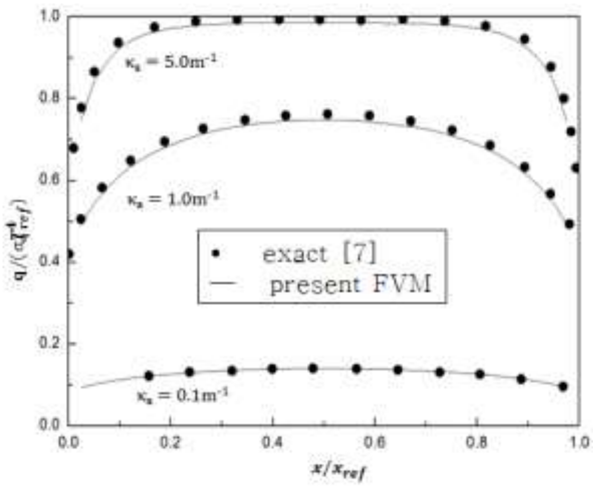

Figure. 3 Comparison of the dimensionless radiative wall heat flux on side wall for three different absorption coefficients, κ_a = 0.1, 1.0 and 5.0 m^{-1}

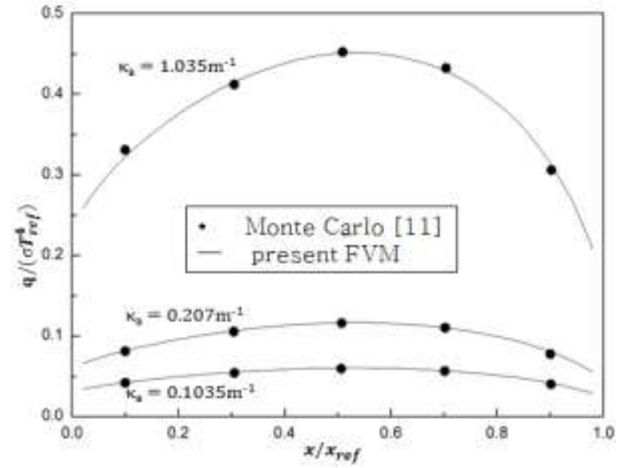

Figure. 4 Comparison of the dimensionless radiative wall heat flux on side wall for three different absorption coefficients, κ_a = 0.1035, 0.207, 1.035 m^{-1}.

TABLE II. Condition of Atmosphere at Several Altitude

h(km)	P_∞ (Pa)	T_∞ (K)	ρ_∞ (Kg/m^3)	n_∞ (m^{-3})	Kn_∞
30	1,197	236.6	0.0180	3.35×10^{23}	6.9×10^{-5}
40	287	250.4	0.0040	7.45×10^{22}	3.4×10^{-4}
50	80	270.7	0.0010	1.86×10^{22}	1.4×10^{-3}
60	22	247.1	0.0003	5.59×10^{21}	5.0×10^{-3}
70	5.2	219.6	0.0008	1.49×10^{21}	1.8×10^{-2}
80	1.0	198.7	0.0002	3.73×10^{20}	7.0×10^{-2}

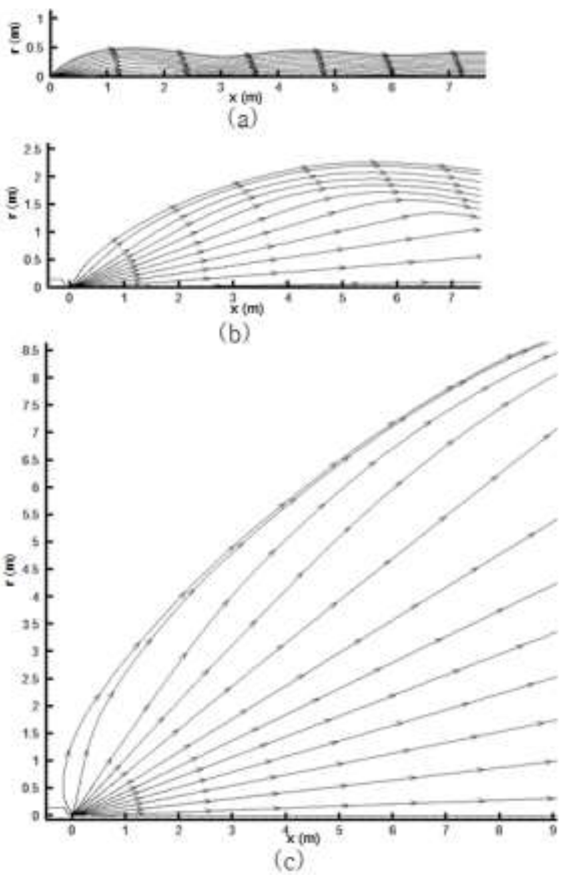

Figure. 5 Plume stream line at (a) 30 km, (b) 50 km, (c) 80 km.

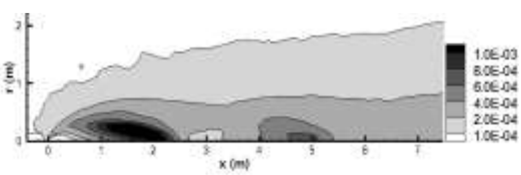

Figure. 6 Local Knudsen number contour at h=30 km.

C. Plume Behavior and Radiative Heat Transfer to the Rocket Base with Altitude

Nozzle of exit radius 3.07 is employed in this study. The nozzle exit pressure is 0.22 MPa, temperature is 1,400 K and the plume is exhausted at Mach 3.2. The conditions of atmosphere varying with altitude are shown in Table 2. Plume stream lines at altitude 30, 50 and 80 km are shown in Fig. 5 to compare the expansion with increasing altitude. The exhausted plume is expanded drastically as altitude increases, and temperature and density inside plume decrease. And, plume near nozzle lip turns more than 90 degree toward upstream as shown in Fig. 5(c). Fig. 6 is Kn contour of h = 30 km plume. Even though the Kn of atmosphere at this altitude falls under the continuum flow regime, local transient region whose Kn is greater than 0.001 is generated due to expansion. Because of this, care is necessary in using the general CFD method to solve this flow though it is relatively low altitude. Fig. 7 is plot of radiative heat flux variation of base surface from the plume as altitude increase. X-coordinate is radius of base and y-coordinate is radiative heat flux. And, Fig. 8 is averaged radiative heat flux of base. X-coordinate is altitude and y-coordinate is radiative heat flux. The radiative heat flux to the base is decrease with increasing altitude. The more expansion of plume with higher altitude results in the more decrease of temperature and density in plume which is radiation source. Temperature distribution of plume near the nozzle and base at h = 30 and 80 km are illustrated in Fig. 9. It shows that the plume temperature distribution at higher altitude is noticeably low. If the plume size get larger the configuration factor between base and plume is increase, and the larger configuration factor promotes the radiation.

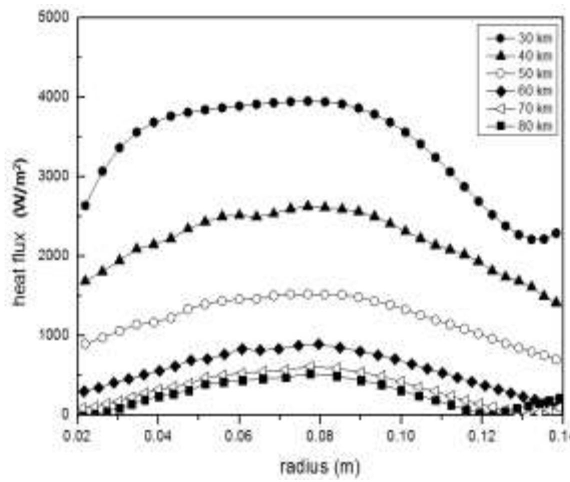

Figure. 7 Radiative heat flux distribution at rocket base.

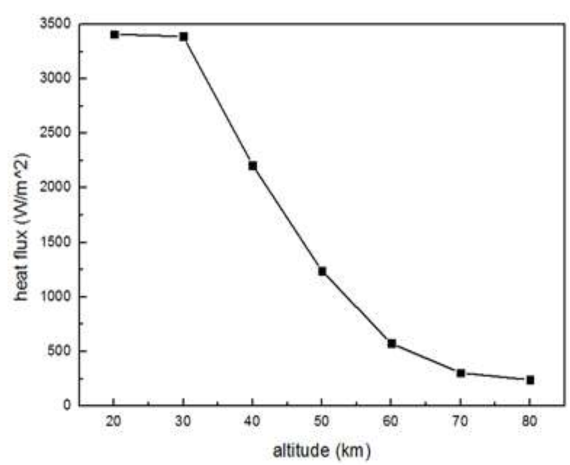

Figure. 8 Averaged radiative heat flux to the base with altitudes.

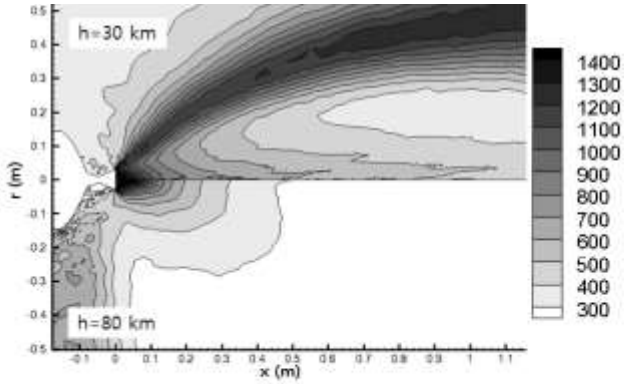

Figure. 9 Temperature contour of plume at h=30 km and 80 km.

However, the decreasing temperature and density have more significant effect on the plume radiation.

IV. Conclusion

In this study, the rocket exhausted plume behavior and resultant radiative heat transfer to the base surface with increasing altitude are analyzed . As altitude increases, the plume is rapidly expanded, and it causes the temperature and density decrease of plume. At h = 30 km, local transient region is generated in the plume due to the rapid expansion and very low density though it is relatively low altitude and Kn of atmosphere is still in continuum flow regime. And lowered temperature and density distribution inside plume with increasing altitude results in the decrease of radiative heat transfer to the base.

Acknowledgment

This research was supported by Agency for Defense Development (ADD), South Korea

References

[1] G. A. Bird, Molecular Gas Dynamics and the Direct Simulation of Gas Flows, Carlendon Press, 1994.

[2] G. A. Bird, "Direct Simulation and the Boltzmann Equation," Phyisics of Fluids, Vol. 13, No. 11, pp. 2676-2681, 1970.

[3] W. Wagner, "A Convergence Proof for Bird's Direct Simulation Monte Carlo Method for the Boltzmann Equation," J. Statistical Physics, Vol. 66, Nos. 3/4, pp. 1011-1044, 1992.

[4] G. A. Bird, "Monte Carlo Simulation in an Engineering Context," Progress in Astonautics and Aeronautics, Vol. 74, pp. 239-255, 1981.

[5] G. A. Bird, "Perception of Numerical Methods in Rarefied Gas Dynamics," Progress in Astronautics and Aeronautics, Vol. 118, pp. 211-226, 1989.

[6] C. Borgnakke, and P. S. Larsen, "Statistical Collision Model for Monte Carlo Simulation of Polyatomic Gas Mixture," J. Comput. Phys., Vol. 18, pp. 405-420, 1975.

[7] J. Y. Murthy and S. R. Mathur, "Radiative Heat Transfer in Axisymmetric Geometries Using an Unstructured Finite-Volume Method," Nume. Heat Transfer B, Vol. 33, p;p. 397-416, 1998.

[8] J. Liu, Shang, H. M. and Chen, Y. S., "Development of an Unstructured Radiation Model Applicable for Two-Dimensional Planar, Axisymmetric, and Three-Dimensional Geometries," J. Quant.Spectrosc. Radiat. Transfer, Vol. 66, pp. 17-33, 2001

[9] M. Y. Kim, "Assessment of the Axisymmetric Radiative Heat Transfer in a Cylindrical Enclosure with the Finite Volume Method," Int. J. Heat Mass Transfer, Vol. 51, pp. 5144-5153, 2008

[10] D. E. Rothe, "Electron-Beam Studies of Viscous Flow in a Supersonic Nozzle," AIAA J., Vol. 9, No. 5, pp. 804-810, 1971.

[11] D. A. Kaminski, "Radiative Transfer from a Gray, Absorbing-Emitting, Isothermal Medium in a Conical Enclosure," J. Solar Energy Eng., Vol. 111, pp. 324-329, 1989.

About Author (s):

Woo Jin Jeon is currently a student of doctoral course in the Department of Aerospace Engineering at KAIST, South Korea